Chin. J. Astron. Astrophys. Vol. 5 (2005), No. 6, 563–570
(*http://www.chjaa.org*)

Chinese Journal of
Astronomy and
Astrophysics

A Composite Model for GHz Peaked Spectra of Radio Sources

Jun Yang[1,2,3], Xiang Liu[1] and Zhi-Qiang Shen[2]

[1] National Astronomical Observatories/Urumqi Observatory, Chinese Academy of Sciences, Urumqi 830011; *junyang@shao.ac.cn*
[2] Shanghai Astronomical Observatory, Chinese Academy of Sciences, Shanghai 200030
[3] Graduate University of the Chinese Academy of Sciences, Beijing 100049

Received 2005 March 3; accepted 2005 November 15

Abstract GHz-Peaked Spectrum (GPS) radio sources are powerful and compact sources with convex spectra. With increasing observational findings, it has been realized that either Synchrotron Self-Absorption (SSA) alone or Free-Free Absorption (FFA) alone is not enough to account for all the spectral features. We present a model consisting of an SSA region partially covered by FFA plasma, and derive a composite spectral formula. By applying the model to a sample of 19 GPS sources having strong absorption, it is found that the external FFA process makes the SSA peak frequency linearly shift to a higher (observed) peak frequency. The shift indicates that the FFA does play a role at the frequency close to the observed peak frequency.

Key words: radio continuum: galaxies — galaxies: active — quasars: general

1 INTRODUCTION

GHz-Peaked Spectrum (GPS) radio sources are a class of compact (< 1 kpc) objects with a convex spectrum peaking between about 0.5–10 GHz. The objects are powerful ($P_{1.4\mathrm{GHz}} > 10^{25}$ W Hz^{-1}) and have low centimeter-wavelength polarization (see the review of O'Dea 1998).

GPS sources make up about 10% of the population of bright radio sources. Optically the GPS sources are a mixed class of quasars and galaxies. The VLBI observations show that most of the GPS galaxies exhibit either a Compact Double (CD) or a Compact Symmetric Object (CSO) morphology (e.g. Stanghellini et al. 2001). The small size and relatively symmetric structure enable us to probe the Narrow Line Region (NLR) and interstellar medium of the host galaxies. The GPS quasars, however, tend to have a core-jet or a complex morphology (e.g. Stanhellini et al. 1999) and have high redshifts. The small size of the GPS sources is likely due to a surrounding dense medium (O'Dea et al. 1991) or an early stage of evolution (Phillips & Mutel 1982; Taylor et al. 2000; Wang et al. 2003). The young sources may evolve through a compact steep-spectrum stage to become large-size radio sources, e.g., FR II (Readhead et al. 1996; Fanti et al. 1995).

The turnover in the spectrum is not well understood at present. Although Synchrotron Self-Absorption (SSA) is widely believed to be responsible for the inverted spectrum, it is also possible that Free-Free Absorption (FFA) plays a role in the high density regions surrounding the source (Bicknell et al. 1997). In this paper, we try to consider a model consisting of an SSA region partially covered by an FFA plasma.

2 SSA VS FFA

Currently the SSA process and the FFA process are the two main competing mechanisms to explain the spectral turnover seen in the GPS sources. The SSA interpretation is mainly based on the following findings. (1) There is an anti-correlation between the intrinsic turnover frequency and the linear size of the sources (O'Dea & Baum 1997; Snellen et al. 2000). (2) The low frequency spectral index[1] $\alpha_{\rm low}$ usually appears to be less than 2.5, as is expected in the SSA model.

However, some other findings can not be interpreted by the SSA mechanism alone. (1) In a few cases, large values of $\alpha_{\rm low}$, e.g. 3.5, in the source 0457+024 (Stanghellini et al. 1998), have been found. (2) The spectral inversion in some sources including OQ 208 (Kameno et al. 2000) is stronger in the receding jet than in the approaching jet. (3) There is no significant evidence for a 90° change in the position angle of polarization across the spectral peak in six sources observed by Mutoh et al. (2002). (4) Optical observations (de Vries et al. 2000; O'Dea et al. 1996; Stanghellini et al. 1993) have shown that many of the GPS sources are located in disturbed or interacting systems, whose nuclear environments may be expected to be dense. Therefore, it seems plausible that the density may be high enough for the FFA to play a role. The FFA has also been found to be operative in a number of GPS sources, e.g., 0108+388 (Marr et al. 2001) and 1946+708 (Peck et al. 1999; Peck & Taylor 2001).

It appears that some of the above findings support the SSA and some support the FFA. To give a comprehensive interpretation we may invoke both processes. Here we construct a composite model and apply it to a sample of 19 GPS sources.

3 A COMPOSITE MODEL

We present a model consisting of an internal SSA and an external FFA. We start with the region emitting synchrotron radiation. For a homogeneous, self-absorbed, and incoherent synchrotron emission region with a power-law electron energy distribution, the spectrum of the radiation (Pacholczyk 1970) is:

$$S_\nu^{\rm s} = S_0 \nu^{2.5} [1 - \exp(-\tau_{\rm s} \nu^{\alpha - 2.5})] \ , \tag{1}$$

where ν is the frequency in GHz, $\tau_{\rm s}$ is the SSA optical depth at 1 GHz and α is the high frequency (optical thin) spectral index. S_0 is a scaling factor and $S_0 \tau_{\rm s}$ is nearly equal to the flux density at 1 GHz if $\tau_{\rm s} \ll 1$.

After leaving the SSA region, the radiation encounters a screen consisting of more or less ionized clouds. For simplicity we assume that the clouds have an uniform opacity. We assume a fraction b (≤ 1) of the radiation which is intercepted by the clouds and is subject to FFA, and the fraction $(1-b)$ of the radiation which is going through the gaps of the clouds. The observed radiation ($S_\nu^{\rm o}$) therefore consists of an FFA-diluted spectrum (fraction b) and an undiluted part (fraction $1-b$),

$$S_\nu^{\rm o} = b S_\nu^{\rm s} \exp(-\tau_{\rm f} \nu^{-2.1}) + (1-b) S_\nu^{\rm s} \ , \tag{2}$$

where $\tau_{\rm f}$ is an average opacity at 1 GHz for all the clouds. Here we omit the spontaneous free-free radiation from the thermal clouds due to the reasons that the radio emission from a

[1] we define spectral index: $S_\nu \propto \nu^\alpha$

source with the brightness temperature $T_{\rm b0}$ propagates through a foreground cloud with electron temperature $T_{\rm e}$. The observed brightness temperature is

$$T_{\rm b} = T_{\rm b0}\exp(-\tau_{\rm f}\nu^{-2.1}) + T_{\rm e}[1-\exp(-\tau_{\rm f}\nu^{-2.1})]. \quad (3)$$

For radio loud AGNs such as GPS sources, $T_{\rm b0}$ is usually $> 10^8$ K, while $T_{\rm e}$ of the foreground cloud is about $\sim 10^4$ K. So the second term of Equation (3), i.e., the free-free radiation, can be omitted.

There are four parameters, $\tau_{\rm s}$, $\tau_{\rm f}$, b, α, and the mere scaling factor S_0 in Equations (1) and (2). If the fraction $b \ll 1$, or if the clouds are optically thin, i.e. $\tau_{\rm f}\nu^{-2.1} \ll 1$, the composite model (Eq. (2)) reduces to the homogeneous SSA model (Eq. (1)). If the SSA region is optically thin and the clouds completely obscure the emitting region, i.e. $b \simeq 1$ and $\tau_{\rm s}\nu^{\alpha-2.5} < 1$, Equation (2) reduces to the uniform FFA model ($S^0_\nu \propto \nu^\alpha \exp(-\tau_{\rm f}\nu^{-2.1})$). If the source is completely optically thin ($\tau_{\rm f}\nu^{-2.1} \ll 1$, $\tau_{\rm s}\nu^{\alpha-2.5} \ll 1$), the observed flux density is $S^{\rm o}_\nu \simeq S_0\tau_{\rm s}\nu^\alpha$.

4 APPLICATION OF THE MODEL

4.1 A GPS Source Sample

We can anticipate that the composite model can give reasonable results when applied to heavily absorbed systems. Therefore, we selected 19 sources (see Table 1) with highly ($\alpha_{\rm low} > 1.5$) inverted spectra from the complete sample (Stanghellini et al. 1998) and the High Frequency Peakers (HFP) sample (Dallacasa et al. 2000). Each source has a steep ($\alpha \leq -0.5$) optically thin spectrum and a minimum of eight data points. The majority of the data were obtained from the quasi-simultaneous muti-frequency observations at the Very Large Array (VLA). The errors in flux density are listed in the Stanghellini sample and estimated 3% at 1.4, 1.7, 4.5, 5.0, 8.1 and 8.4 GHz, 5% at 15 GHz and 10% at 22.5 GHz in the HFP sample.

4.2 Spectral Fitting

For numerical fitting to the observed spectrum, we rewrite Eq. (2) in the form:

$$S^{\rm o}_\nu = S_1\nu^{2.5}[1-\exp\left(-\tau_{\rm s}\nu^{\alpha-2.5}\right)][r+\exp\left(-\tau_{\rm f}\nu^{-2.1}\right)] \ , \quad (4)$$

where we define $r = (1-b)/b$ and $S_1 = bS_0$. We have developed a program to fit the spectral data with the function Nonlinear Regress in the Mathematica software package Statistics[2]. The function minimizes the merit function $\chi^2 = \sum_{i=1}^{n}[(y_i - y)^2/\sigma_i^2]$ (y_i the observed flux, y the model value and σ the error) with the Levenberg Marquardt method (Bates & Watts 1988). After we obtained the best fit of the parameters (S_1, $\tau_{\rm s}$, α, r, and $\tau_{\rm f}$), we homed in on the peak frequency $\nu^{\rm s}_{\rm m}$ of the SSA spectrum $S^{\rm s}_\nu$ and the peak frequency $\nu^{\rm o}_{\rm m}$ of the FFA modified spectrum $S^{\rm o}_\nu$ by with the function NMaximize. There are six effective digits of precision in the final result. We have tried the pure homogenous SSA model and the pure uniform FFA model, both fits have quite large deviations from the observed data, which indicate the necessity of a composite model.

5 RESULTS AND DISCUSSION

The spectral fitting results are displayed in Figure 1. In each panel, the curve is the best fit and the data points are marked with their 3-σ error bars. For two sources 0019−000 and 0500+019, the points at the highest frequency were not used in the fitting process because it seems to indicate a spectral break. The break is possibly due to synchrotron radiation loss.

[2] http://documents.wolfram.com/mathematica /Add-onsLinks/StandardPackages/Statistics

Table 1 Model fit parameters of the spectra. Col. (1), B1950 IAU name; Col. (2), redshift; Col. (3), optical identification, G: galaxy, Q: quasar; Col. (4), spectral index of low frequency; Cols. (5–9), estimated values of the fit parameters of the composite model; Col. (10), reduced chi-square (dof: degree of freedom, dof = 5); Col. (11), fraction of the radiation meeting the clouds; Col. (12), peak frequency of the SSA spectrum $S_\nu^{\rm s}$ in GHz; Col. (13), peak frequency of the FFA modified spectrum $S_\nu^{\rm o}$ in GHz.

Source	z	id	$\alpha_{\rm low}$	S_1	$\tau_{\rm s}$	$\tau_{\rm f}$	r	α	χ^2/dof	b	$\nu_{\rm m}^{\rm s}$	$\nu_{\rm m}^{\rm o}$
(1)	(2)	(3)	(4)	(5)	(6)	(7)	(8)	(9)	(10)	(11)	(12)	(13)
0019−000	0.305	G	1.65	76.63	0.04	0.63	0.70	–0.90	0.424	0.59	0.44	0.76
0034+078			1.84	0.12	9.93	16.67	0.33	–0.79	0.033	0.75	2.45	5.15
0108+388	0.668	G	2.06	1.10	17.02	20.84	0.16	–1.37	0.030	0.86	2.19	4.61
0237−233	2.223	Q	1.93	17.73	0.18	1.61	2.10	–0.66	1.629	0.32	0.74	0.86
0457+024	2.384	Q	3.56	5.19	0.59	3.39	0.59	–0.66	0.934	0.63	1.09	2.30
0500+019	0.583	G	2.48	16.07	0.20	1.97	0.49	–0.56	0.913	0.67	0.80	2.04
1143−245	1.950	Q	2.53	7.16	0.49	4.24	0.49	–0.77	0.005	0.67	0.99	2.40
1333+459	2.449	Q	1.72	0.40	9.46	14.01	0.30	–0.95	0.002	0.77	2.21	4.35
1333+589			1.64	0.20	7.64	17.27	0.67	–0.58	0.143	0.60	2.60	5.31
1358+624	0.431	G	1.49	285.48	0.01	0.22	0.68	–0.75	0.402	0.60	0.32	0.57
1404+286	0.077	G	1.60	1.58	9.20	18.03	0.24	–0.96	0.626	0.80	2.18	4.97
1427+109	1.710	Q	1.96	0.17	6.39	6.85	0.79	–0.39	0.294	0.56	2.93	4.61
1509+054		G	2.09	0.17	10.23	25.67	0.18	–0.36	0.670	0.84	3.60	10.15
1607+268	0.473	G	1.63	147.05	0.05	0.73	0.25	–1.07	0.663	0.80	0.49	1.01
1614+051	3.197	Q	1.50	0.58	8.28	14.31	0.30	–0.99	0.180	0.77	2.09	4.27
1848+283	2.560	Q	1.52	1.04	7.34	27.84	0.10	–0.66	0.126	0.91	2.42	8.06
2008−068		G	2.17	44.86	0.09	1.36	0.40	–0.86	0.350	0.71	0.57	1.38
2128+048	0.990	G	1.72	85.92	0.05	1.57	0.69	–0.84	2.872	0.59	0.50	0.51
2201+098			2.06	0.29	17.21	24.75	0.17	–1.36	0.480	0.86	2.20	4.96

The best-fit parameter values are listed in Table 1 (Cols. 5–9). Column (10) gives the values of the reduced chi-squared χ^2/dof, some are much less than 1 probably due to the over-estimated error bars. There seems a kind of small concavity near the peak of the fit spectrum of some sources, i.e., 1848+283, 2008+068, 2128+048 and 2201+098, though the fit spectra are closer to their observed data. The model-fit spectrum is the sum of the two peaked spectra, i.e., the SSA spectrum and the FFA-diluted SSA spectrum, so it may appear a concavity between the two separate peaks. However, the actual spectrum at the concavity is likely to be smoother than our fit curve. The imperfection may be because the average FFA opacity for the clouds is unable to represent completely a certain range of opacities. The inhomogeneity in the radiation region may also make the spectra flatter to some extent.

In the composite model, the FFA makes the peak of the spectrum bS_ν^s shift to a higher frequency. The unshifted peak frequency $\nu_{\rm m}^{\rm s}$ of the spectrum $(1-b)S_\nu^s$ could be the lower limit of the observed peak frequency. Figure 2 displays the shift of the peak frequencies which are distributed above the dotted line (the lower limit $\nu_{\rm m}^{\rm o} = \nu_{\rm m}^{\rm s}$), as the composite model expects. A linear correlation between the two kinds of peak frequencies is indicated, when we fit them with a straight line:

$$\nu_{\rm m}^{\rm o} = (-0.38 \pm 0.44) + (2.45 \pm 0.23)\nu_{\rm m}^{\rm s} \ . \qquad (5)$$

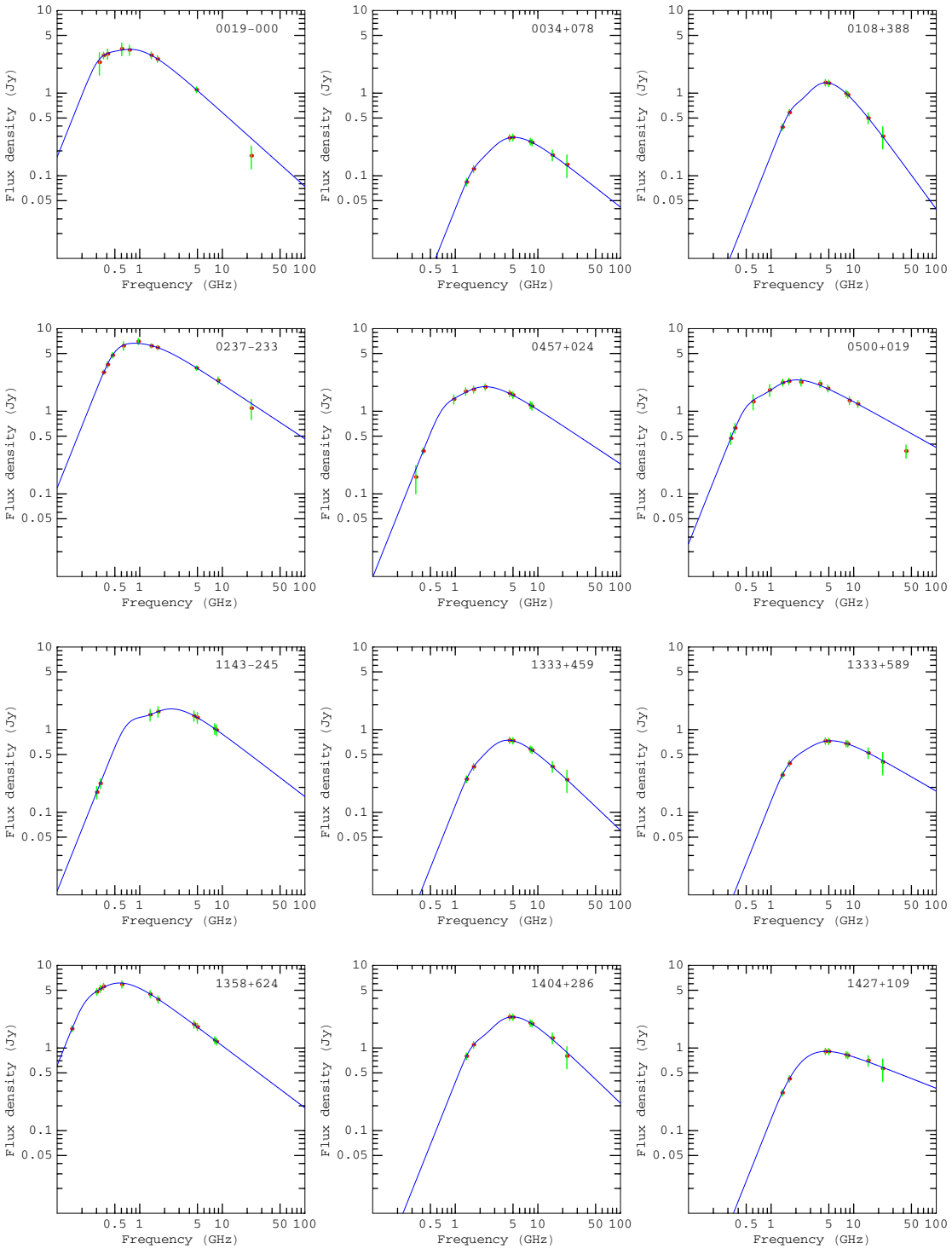

Fig. 1 Spectral fitting of 19 GPS sources with the composite model. The solid lines represent the best fits. The full length of error bars corresponds to 6σ. The flux data were obtained from the complete sample (Stanghellini et al. 1998) and the HFP sample (Dallacasa et al. 2000).

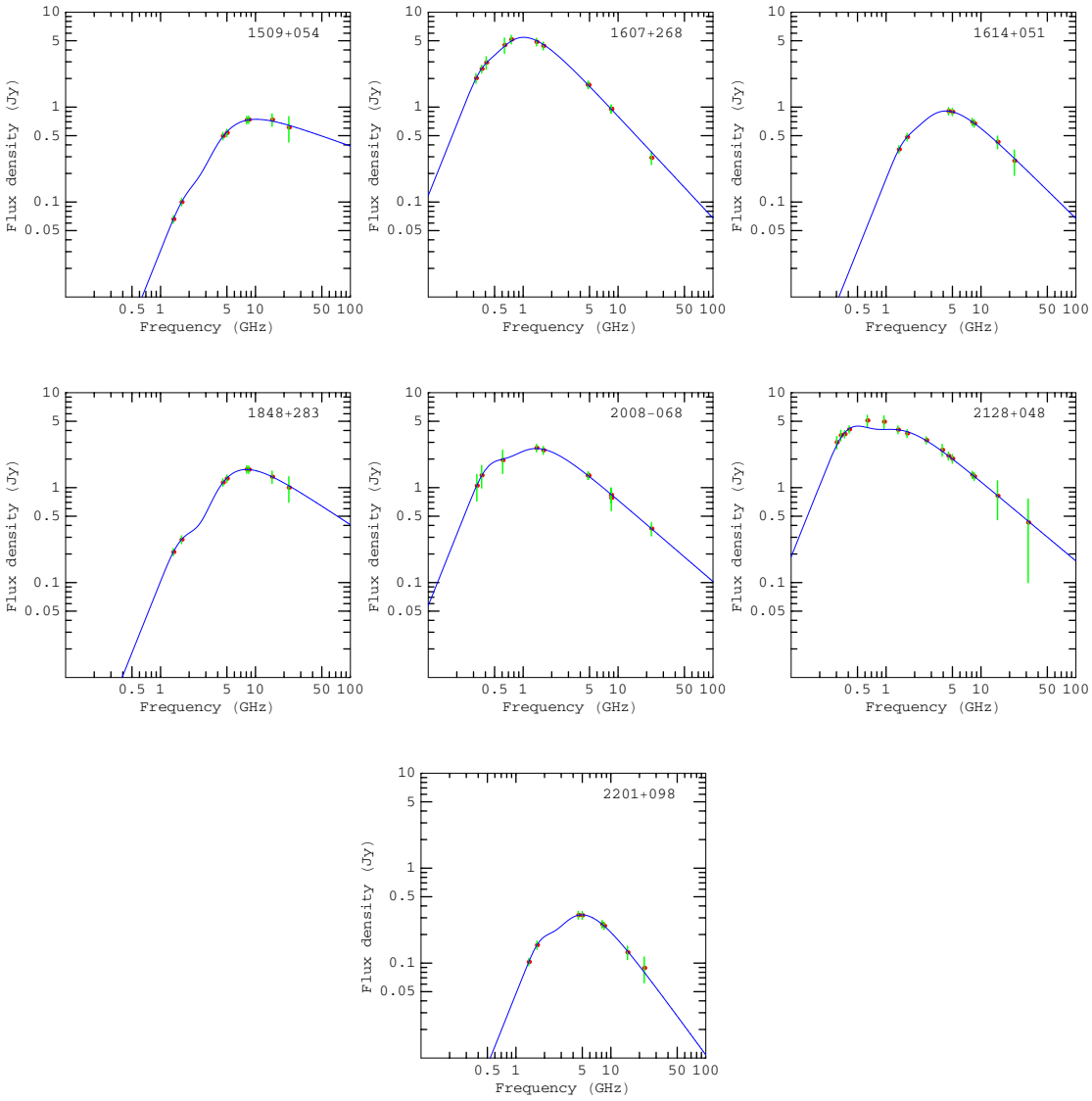

Fig. 1 Continued.

The correlation coefficient R=0.9328, the standard deviation SD = 0.9827, and the probability (that R is zero) $P < 0.0001$. The shift indicates that the FFA does play a role at frequencies close to the observed peak frequency. In the case that the optical depth τ at the peak frequency $\nu_{\rm m}$ is approximately equal to 1, and the SSA peak frequency $\nu_{\rm m}^{\rm s}$ can be written as $\nu_{\rm m}^{\rm s} \approx (\tau_{\rm s})^{\frac{1}{2.5-\alpha}}$. At the frequency $\nu > \nu_{\rm m}^{\rm s}$, the internal radiation region is optical thin. So the observed peak frequency can be estimated by $\nu_{\rm m}^{\rm o} \approx \nu_{\rm m}^{\rm f} \approx (\tau_{\rm f})^{\frac{1}{2.1}}$. Therefore, the correlation may originate from $(\tau_{\rm s})^{\frac{1}{2.5-\alpha}} \propto (\tau_{\rm f})^{\frac{1}{2.1}}$, which means that there may exist a physical dependence between the FFA region and the synchrotron radiation region.

In a uniform FFA plasma, the electron density can be estimated from (see e.g. O'Dea 1998)

$$n_{\rm e}^2 L \simeq 3.05 \times 10^6 \tau_{\rm f} T_4^{1.35} \ , \qquad (6)$$

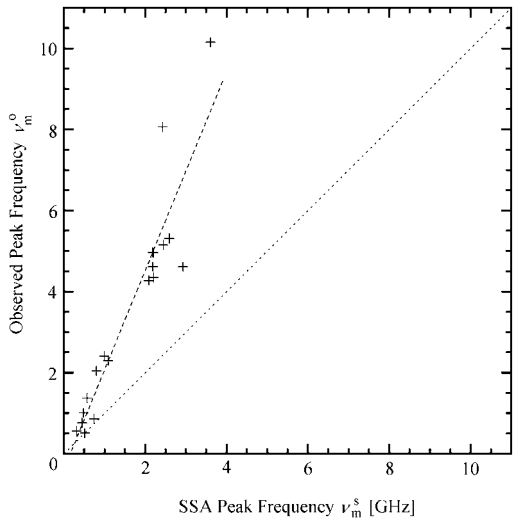

Fig. 2 Observed peak frequency vs SSA peak frequency for 19 sources. The dashed line is a linear fit: $\nu_{\rm m}^{\rm o} = (-0.38 \pm 0.44) + (2.45 \pm 0.23)\nu_{\rm m}^{\rm s}$. The dotted line is the lower limit: $\nu_{\rm m}^{\rm o} = \nu_{\rm m}^{\rm s}$.

where $n_{\rm e}$ is the electron density in cm^{-3}, T_4 is the electron temperature in 10^4 K, and L is the thickness of the plasma along the line of sight in pc. If we take $T_4 = 1.6$, a typical temperature for an NLR (Koski 1978) and $\tau_{\rm f} = 0.18 \sim 27.84$ which is obtained from the composite model, then the emission measure $n_{\rm e}^2 L$ is of $1.0\times10^6 \sim 1.6\times10^8$ cm^{-6} pc. Take $L = 100$ pc, a typical size for GPS sources, we obtain the electron densities in the range 1.0×10^2 cm^{-3} $\sim 1.3 \times 10^3$ cm^{-3}. This is consistent with the measured range ($n_{\rm e} = 10^2 \sim 10^4$ cm^{-3}) with the [S II] doublet for the NLR (Koski 1978).

The images of the NVSS (NRAO VLA sky survey, 45 arcsecond beam) show that all the sources except two are compact point sources. The source 2008+051 appears to be slightly resolved with an elliptical shape. The other source 1614+051 has a strong component and a possible weak jet. All the sources except 0034+073 have VLBI observations at some frequencies and the VLBI images show some small scale components. The components' spectra are unavailable for us because of the lack of multi-frequency VLBI observations. However, the main components' spectra of each source may tend to have similar shape and their peak frequencies may tend to be located in a small range due to the restriction of selecting spectra with $\alpha_{\rm low} > 1.5$ and $\alpha \leq -0.5$. So it is reasonable to apply the composite model to the total power spectra to obtain a rough description of the sources at this stage. A component spectral analysis with the composite model is expected in the future.

6 SUMMARY AND CONCLUSIONS

The observational findings of the GPS sources cannot be well explained by a pure SSA model or a pure FFA model. We propose a model consisting of an internal SSA and an external partial FFA. Based on the assumption of a homogeneous SSA region covered partially by some uniform-opacity ionized clouds, a composite spectral formula have been developed.

We have applied the model to a sample consisting of 19 GPS sources with heavily ($\alpha_{\rm low} > 1.5$) absorbed spectra. The fit curves indicate that the composite model is a better description of the sources' spectra. It is found that the external FFA process makes the SSA peak frequency shift linearly to a higher (observed) peak frequency in our sample. The shift indicates that the FFA plays a role at the frequency close to the observed peak frequency.

Acknowledgements We thank Professors Tao Kiang and Richard Strom for valuable comments. This research has made use of the NASA's Astrophysics Data System, and the NASA/IPAC Extragalactic Database (NED) which is operated by the Jet Propulsion Laboratory, California Institute of Technology, under contract with the National Aeronautics and Space Administration.

References

Bates D. M., Watts D. G., 1988, Nonlinear Regression Analysis and Its Applications, New York: John Wiley & Sons
Bicknell G. V., Dopita M. A., O'Dea C. P., 1997, ApJ, 485, 112
Dallacasa D., Stanghellini C., Centonza M., Fanti R., 2000, A&A, 363, 887
de Vries W. H., O'Dea C. P., Barthel P. D. et al., 2000, AJ, 120, 2300
Fanti C., Fanti R., Dallacasa D. et al., 1995, A&A, 302, 317
Kameno S., Horiuchi S., Shen Z. Q. et al., 2000, PASJ, 52, 209
Koski A. T., 1978, ApJ, 223, 56
Marr J. M., Taylor G. B., Crawford F. III, 2001, ApJ, 550, 160
Mutoh M., Inoue M., Kameno S. et al., 2002, PASJ, 54, 131
O'Dea C. P., 1998, PASP, 110, 493
O'Dea C. P., Baum S. A., 1997, AJ, 113, 148
O'Dea C. P., Baum S. A., Stanghellini C., 1991, ApJ, 380, 66
O'Dea C. P., Stanghellini C., Baum S. M., Charlot S., 1996, ApJ, 470, 806
Pacholczyk A.G., 1970, Radio Astrophysics, San Francisco: Freeman
Peck A. B., Taylor G. B., 2001, ApJ, 554, L147
Peck A. B., Taylor G. B., Conway J. E., 1999, ApJ, 521, 103
Phillips R. B., Mutel R. L., 1982, A&A, 106, 21
Readhead A. C. S., Taylor G. B., Pearson T. J., Wilkinson P. N., 1996, ApJ, 460, 634
Snellen I. A. G., Schilizzi R. T., Miley G. K. et al., 2002, MNRAS, 319, 445
Stanghellini C., Dallacasa D., O'Dea C. P. et al., 2001, A&A, 377, 377
Stanghellini C., O'Dea C. P., Murphy D. W., 1999, A&AS, 134, 309
Stanghellini C., O'Dea C. P., Baum S. A., 1993, ApJS, 88, 1
Stanghellini C., O'Dea C. P., Dallacasa D. et al., 1998, A&AS, 131, 303
Taylor G. B., Marr J. M., Pearson T. J. et al., 2000, ApJ, 541, 112
Wang W. H., Hong X. Y., An T., 2003, ChJAA, 3, 505